MEASUREMENTS IN LOW LATITUDE HIGH ALTITUDE CIRRUS

Andrew J. Heymsfield, Carl Schmitt and Aaron Bansemer
National Center for Atmospheric Research
Boulder, Colorado

1. INTRODUCTION

According to the ISCCP definition, optically thin ice clouds–cirrus, are those which have optical depths (τ) below 3.6. Thicker cirrus–cirrostratus, have optical depths between 3.6 and 23. Each cirrus type traps the same amount of long wave radiation emitted from the earth's surface (Hartmann et al. 1983, for τ above and below 10). However, the more numerous thin ice clouds reflect relatively little incoming solar radiation whereas the opposite is true for thick cirrus. The resulting net radiative flux divergence (longwave minus shortwave) of thin cirrus is positive whereas that of thicker cirrus is negative (Hartmann et al., 1983).

Ice particle fallspeeds are central in determining the longevity of ice clouds and therefore how they influence the earth's radiation budget. Particle size distributions are not yet predicted directly in climate models, ice particle fallspeeds in ice clouds are parameterized using very general assumptions about the shapes and size distributions of the component particles. Furthermore, the fallspeeds in models are not size dependent, but are represented in terms of the ensemble mean particle fallspeed, V_m. The V_m are represented in terms of a bulk property of the PSD, the ice water content (IWC) or the ice water mixing ratio. As shown in Fig. 1, there is a wide variability amongst V_m-IWC relationships. Figure 2 shows that there is a strong dependence of the earth's net radiation budget in climate models on the assumed or parameterized V_m.

* *Corresponding author address:* Andrew Heymsfield, NCAR/MMM, 3450 Mitchell Lane, Boulder, CO 80303; e-mail: heyms1@ncar.ucar.edu

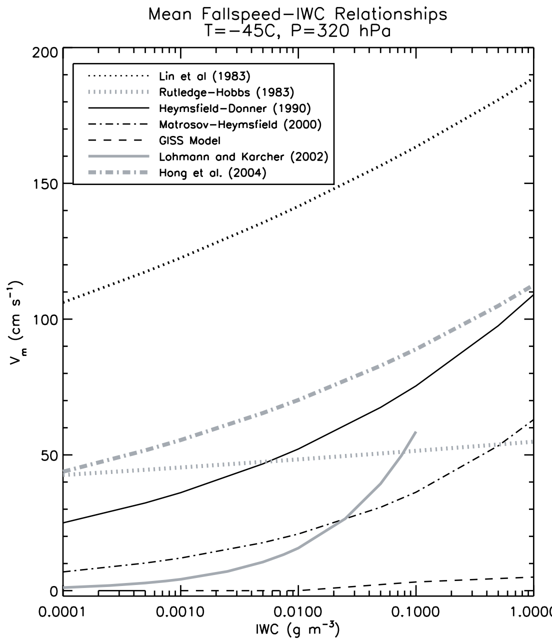

Fig. 1: Relationship between V_m and IWC from the investigators noted, for approximately the temperature and pressure levels shown. Velocities for the ECHAM 5 model (Lohmann and Karcher, 2002) assume pressure of 400 hPa, temperature -40°C , and a number concentration of 0.1 cm^{-3}.

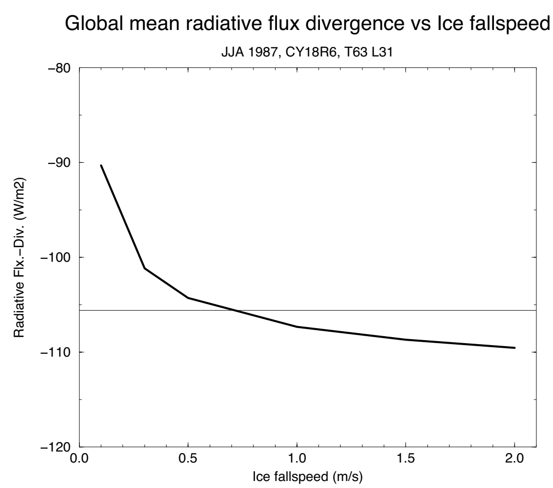

Figure 2. Average net global flux divergence for the period June, July, and August 1987 as derived by the ECMWF model by C. Jakob (private communication). The horizontal line is the model control integration derived using the Heymsfield and Donner

(1990) V_t vs. X_{IWC} representation. Figure from Heymsfield and Iaquinta (2000), courtesy C. Jakob, ECMWF.

In this study, we provide new information on the particle size distributions (PSD) and IWC for low latitude cirrus in the temperature range -40C to -85°C . The PSD are measured using electronic probes, augmented by data from impactor-type probes to provide improved information in the size range of 10 to 100 μm that is difficult to measure with the electronic probes alone. We also show that high concentrations of sub-micron solution droplets may be present in cold, low latitude cirrus in the vicinity of convection. Section 2 identifies the data sources and instrumentation. In Section 3, we show the microphysical properties and ensemble-mean fall velocities of low latitude maritime, convectively generated clouds forming either through deep convection or in-situ. Section 4 shows data from an aircraft icing event at low temperatures. Section 5 summarizes the results.

2. DATA SETS AND INSTRUMENTATION

Data examined here were acquired in ice clouds in low latitude, maritime locations with and without continental influences. Recent data were collected during the Cirrus Regional Study of Tropical Anvils and Cirrus Layers Florida Area Cirrus Experiment (CRYSTAL-FACE, 2002, Florida, hereafter CF), the Aura Validation Experiment (pre-AVE, 2004, Costa Rica), the Aerosol and Chemical Transport in Tropical Convection (ACTIVE, Darwin, Dec. 2005) and the Tropical Warm Pool International Cloud Experiment (TWP-ICE, Darwin, Jan.-Feb. 2006). flights that were conducted on 21 days in ACTIVE, nine days in CF, and one day in pre-AVE. The primary sampling aircraft for CF and pre-AVE was the NASA WB57F, and for Darwin was the University of Flinders Egrett. The clouds sampled were convective or perturbed by convection in each experiment, except for thin to subvisual cirrus in pre-AVE and for a subset of clouds in CF.

Size-spectra measurements were obtained in sizes from about 0.5 to 1,500 μm with Droplet Measurement Technologies' (DMT) Cloud Aerosol and Precipitation Spectrometer (CAPS, Baumgardner et al. 2005) 2D-C type Cloud Imaging Probe (CIP). The CIP resolution was about 25 μm. "Reconstruction" of partially imaged particles increased the maximum dimension to 2,000 μm. The Droplet Measurement Technologies' Cloud and Aerosol Spectrometer (CAS) on the CAPS measured PSD in the 0.5 to 50 μm size range in 30 bins, although only when small particles predominate could the measurements be free of artifacts produced by the breakup of large crystals on the probes' inlet. Data were averaged over 5 second intervals, or about from 0.5 to 1 km of horizontal flight distance.

Our video ice particle sampler (VIPS), an impactor type device (Heymsfield and McFarquhar, 1996), augmented information on the PSDs and particle cross-sectional areas in the size range from 10 to 200 μm. The VIPS was used to collect data in thin cirrus during CF and pre-AVE at temperatures -50°C and below, where significant numbers of particles may have been below sizes ($\approx$100 μm) adequately sampled by the imaging probes and above the size range measured by the CAS. The VIPS collects ice particles larger than 10 to 20 μm in size, and provides detailed imagery of the particles with a resolution of a few microns. The VIPS data analysis was done semi-automatically, with the software trained manually and thoroughly evaluated objectively.

Ice water content was measured directly by total water content (TWC) probes, the University of Colorado (CU) probe and the Harvard probe (Weinstock et al., 1994). The Harvard probe is more suitable for higher IWC sampling and is used for most of the CF observations and those during pre-AVE where the CU instrument was not available. Intercomparison of the the CU and Harvard instruments in low IWC regions during CF and a more recent field program (Mid-continental Cirrus Experiment, MidCiX) suggest that the CU instrument has better sensitivity at low IWC. Accordingly, the CU instrument is used for low temperature, low IWC regions during CF.

3. RESULTS

The maximum measured particle diameter of the particle size distributions (PSDs), D_{max}, generally decreased with decreasing temperature (Fig. 3). For temperatures above -50°C , peak sizes in the Darwin and CF clouds often reached the maximum measurable diameter of 2 mm (Figs. 3a and b). The D_{max} showed an increase from -70 to -85°C for the Darwin data (Fig. 3a), which, because the sizes were so large, signified that the cold clouds sampled were increasingly the direct result of convection. The results for the CRYSTAL-FACE data set were similar, with the majority of points, in temperatures from -50 to -70°C , having D_{max} that are similar to the Darwin data. The lowest values of D_{max} were observed in the thin cirrus (Fig. 3c).

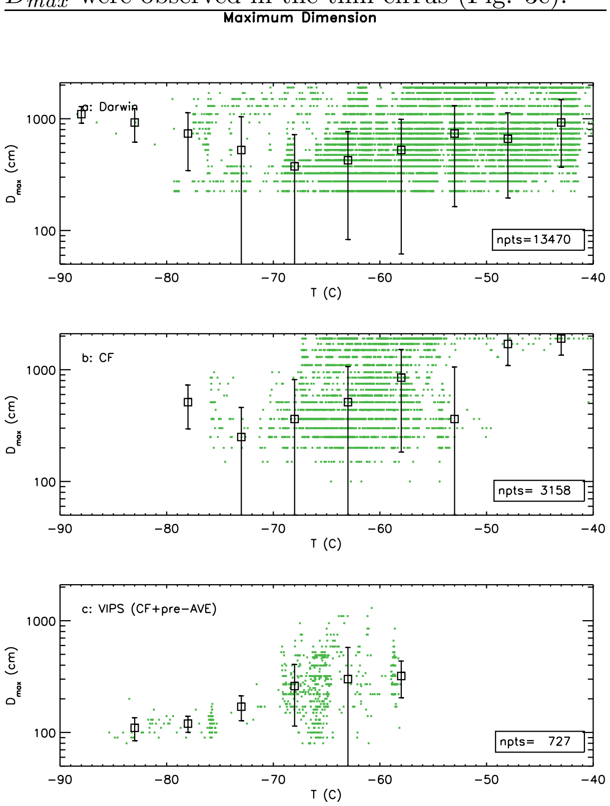

Figure 3. Maximum dimension of particles as a function of temperature, for the a: Darwin, b: CRYSTAL-FACE, and c: low temperature CRYSTAL-FACE and pre-AVE data sets, using data from the NCAR video ice particle sampler (VIPS). Each point represents one 5-sec particle size distribution. The number of points in each data set are shown.

In the absence of deep convection, and with relatively weak updrafts, the ice water content is given roughly by the difference in the vapor density at water and ice saturation, the Bergeron-Findeisen (B-F) process. Homogeneous ice nucleation limits the peak ice supersaturation to about 60%. Curves representing the IWC-temperature dependence with these criteria are plotted in each of the panels of Fig. 4. The figure also shows the temperature dependence of the observed IWC for each of the data sets from Fig. 3. It is noted that the IWCs from the Darwin data set (Fig. 4a) for temperatures -50°C and below are one to two orders of magnitude higher than the B-F amount. The median value of the IWC increases from -70 to -85°C , from which it can be concluded that the penetrations were in the immediate vicinity of convection. The IWCs for Darwin and CAF may be underestimated by a small amount due to the absence of measurements above 2 mm in size. The CF IWCs are lower than those from the Darwin clouds, and in the mean are near the B-F curve (Fig. 4b). For the thin cirrus, dominated by clouds produced by weak, shallow updrafts, the IWCs are bounded by the B-F amount (Fig. 4c). Shown for comparison in Fig. 4c are IWCs derived from the VIPS probe from CEPEX (Heymsfield and McFarquhar, 1996), which are also bounded by the B-F amount. From Fig. 4, we conclude that the Darwin IWCs were mostly dominated by transport from deep convection, many of the CF samples were also dominated by convection, and the thin cirrus were the result of in-situ generation.

Gamma equations of the form $N = N_0 D^{\mu} e^{-\lambda D}$ were fitted to the PSD over sizes(D) measured by the 2D probes, as in Heymsfield et al. (2002). The slope of the PSD, λ, is a strong function of temperature (Fig. 5). The decrease in λ values at temperatures below about -70°C in the Darwin data set further supports the view that the low-temperature Darwin samples were in clouds where particles had recently been lofted from below. We found that λ for the Darwin data reached a minimum of about 40 cm^{-1} and would have clearly been lower had a probe been available to measure to larger sizes.

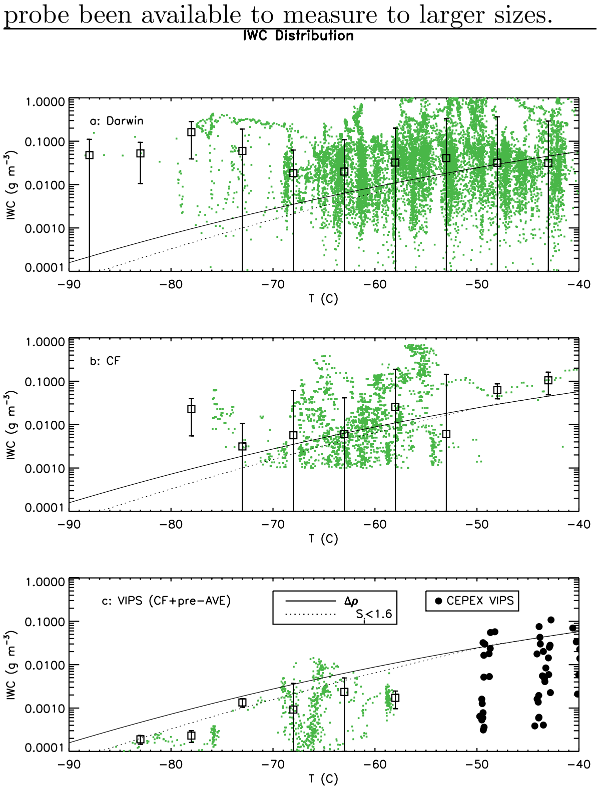

Figure 4. Same as Fig. 3, except for ice water content. In a:, the IWCs are calculated from the particle size distributions and in b: and c:, the IWCs are measured using the University of Colorado total water content probe. Curves representing the Bergeron-Findeisen IWC amount, without and with invoking homogeneous ice nucleation to cap the ice supersaturation, are shown.

The gamma distributions fitted to the VIPS data used a combination of CAS, VIPS, and CIP data. In these instances, few particles were sampled by the CIP to produce reliable gamma fits. The λ values are considerably higher than those from Darwin and CF, signifying formation through in-situ production.

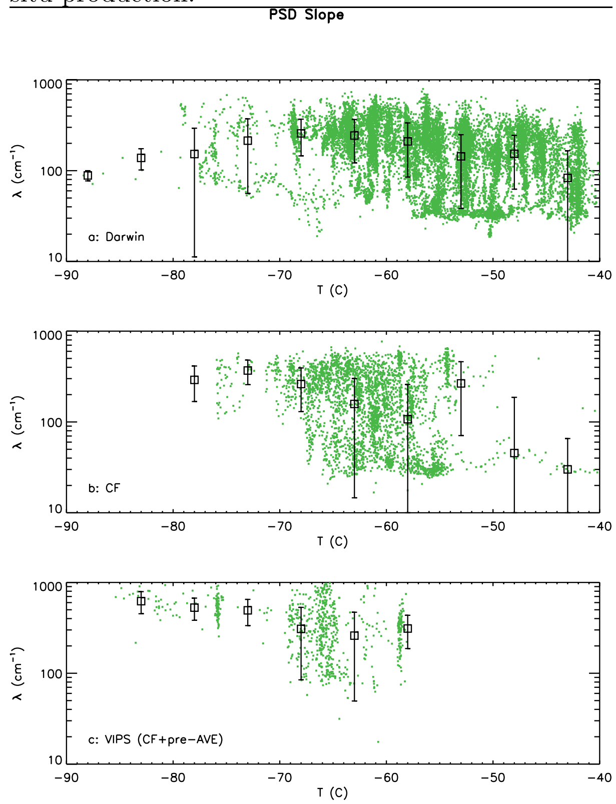

Figure 5. Slope of the gamma particle size distribution fitted to a:, b: particles in 2-D imaging probe sizes, and c: to the entire PSD.

The median values of μ from all three data sets were nearly 0 for all temperatures, although there is considerable scatter noted about the median values (Fig. 6). There does appear to be a tendency for μ to increase slightly with temperature in the CF and thin cirrus clouds. Nonetheless, the observation that μ is nearly 0 is important because it suggests that the PSD can be represented adequately by exponential functions, a feature of the PSD that should simplify the development or parameterizations at these low temperatures.

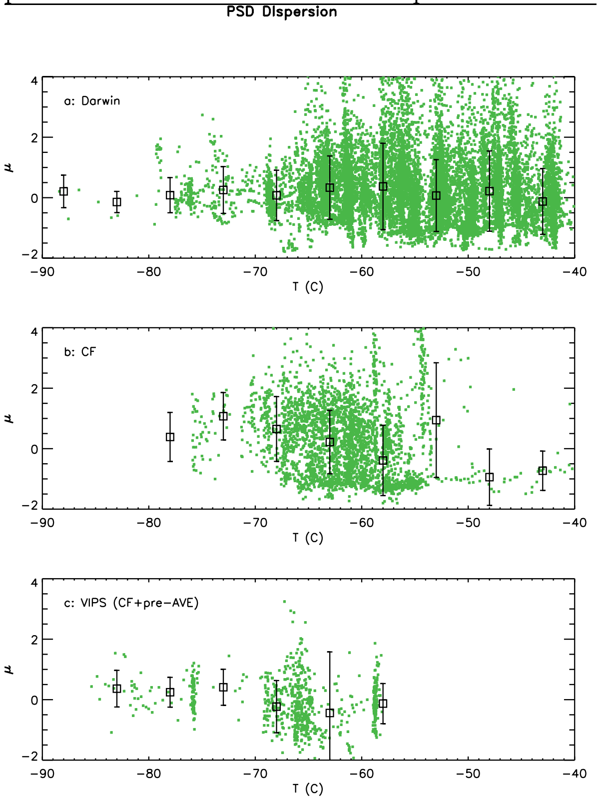

Figure 6. Same as Fig. 5, except that the dispersion μ of the PSD is shown.

4. HIGH CAS CONCENTRATIONS: AIRCRAFT ICING AT -50°C ?

On three occasions during the Darwin experiment, the onboard scientist noted icing on the nacelle, the casing of the aircrafts' turbine engine that covers the Egrett's gearbox, generator, blade hub, and other parts. The scientist noted icing following gradual loss of airspeed, an event likely to be triggered by the icing event. The temperatures were in the -50 to -55°C range and were associated with high concentrations of particles measured by the CAS, of order 50 to 100 cm^{-3}.

Fig. 7 shows a color rendition of the particle size distributions observed on 9 December 2005 when the Egrett encountered two of the events: One at 1512, and another at 1553 (local times). Upon takeoff and landing, at 1400 and 1730, high concentrations of particles, presumably aerosols, were noted in the boundary layer. Also as noted in the figure, high concentrations of particles were observed in the 0.5 to 1.0 micron range, amounting to a total concentration of order 100 cm^{-3}. Because most of the other twenty flight days did not show such events and the times of the high concentrations are consistent with the report of icing, we conclude that highly supercooled, concentrated haze droplets, in the 0.5 to 1 μm range, were responsible for the aircrafts' icing.

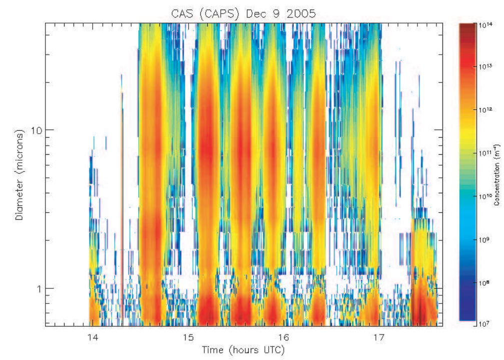

Figure 7. Rendition of particle size distributions measured by the DMT CAS probe on the Egrett aircraft at Darwin on 9 December 2005. Concentration is normalized for bin width, in units of m^{-4}.

5. SUMMARY AND CONCLUSIONS

This study has sought to improve knowledge of the properties of ice particle ensembles found in cold ice clouds found in low latitude regions. The following are some main points:

• The size distributions are approximately exponential

• The PSD slope decreases with temperature but is strongly influenced by transport of condensate from below in the convectively generated ice cloud layers.

• The IWCs in the convectively generated ice cloud are one to two orders of magnitude larger than those found in the thin cirrus, presumably formed by weak uplift.

• Aircraft icing by highly supercooled, presumably highly concentrated haze droplets was observed. The temperatures were in the -50 to -55°C range. This result may explain earlier observations of aircraft icing in hurricanes at temperatures below the point of homogeneous freezing of activated cloud droplets.

Acknowledgments

The authors wish to thank the researchers involved in the Darwin Egrett flights, during ACTIVE and TWP-ICE, for their help in the acquisition of this data. Special thanks go to Geraint Vaughan and Paul Connolly of the University of Manchester/UMIST. Thanks go to Bruce Anderson and Haflidi Jonsson for allowing us to use their CAPS probes.

REFERENCES

Baumgardner, D., H. Chepfer, G. B. Raga, and G. L. Kok 2005: The shapes of very small cirrus particles derived from in situ measurements. *Geophys. Res. Let.*, **32**, L01806, 2005. doi:10.1029/2004GL021300.

D. L. Hartmann, M. E. Ockert-Bell, and M. L. Michelsen, 1992: The effect of cloud type on earth's ergy balance: Global analysis. *J. Cli.*, **5**, 1281-1304.

Heymsfield, A. J., and L. J. Donner, 1990: A scheme for parameterizing ice cloud water content in general circulation models. *J. Atmos. Sci.*, bf 47, 1865-1877.

——, and Greg M.McFarquhar. 1996: High Albedos of Cirrus in the Tropical Pacific Warm Pool: Microphysical Interpretations from CEPEX and from Kwajalein, Marshall Islands. *J. Atmos. Sci.*, **53**, 24242451.

——, and J. Iaquinta, 2000: Cirrus crystal terminal velocities. *J. Atmos. Sci.*, **58**, 916–938.

——, A. Bansemer, P. R. Field, S. L. Durden, J. Stith, J. E. Dye, W. Hall and T Grainger, 2002: Observations and parameterizations of particle size distributions in deep tropical cirrus and stratiform precipitating clouds: Results from in—situ observations in TRMM field campaigns. *J. Atmos. Sci.*, **59**, 3457–3491.

——, C. G. Schmitt, A. Bansemer, D. Baumgardner, E. M. Weinstock, J. T. Smith, and D. Sayres, 2004b: Effective ice particle densities for cold anvil cirrus. *Geophys. Res. Ltrs.*, **31**, L02101.

Lohmann U., and B. Krcher, 2002: First interactive simulations of cirrus clouds formed by homogeneous freezing in the ECHAM general circulation model. *J. Geophys. Res.*, **107** (D10), doi:10.1029/2001JD000767, 2002.

W. B. Rossow and R. A. Schiffer, 1991: ISCCP cloud data products. *Bull. Amer. Meteor. Soc.*, **72**, 2-20.

Weinstock, E. M., E. J. Hintsa, A. E. Dessler, J. F. Oliver, N. L. Hazen, J. N. Demusz, N. T. Allen, L. B. Lapson, and J. G. Anderson, (1994): New fast response photofragment fluorescence hygrometer for use on the NASA ER-2 and the Perseus remotely piloted aircraft, *Rev. Sci. Instrum.*, **65**, 35443554.